

See discussions, stats, and author profiles for this publication at: <https://www.researchgate.net/publication/237058779>

Roles of Free Radicals in Type 1 Phototherapeutic Agents: Aromatic Amines, Sulfenamides, and Sulfenates

ARTICLE in THE JOURNAL OF PHYSICAL CHEMISTRY A · JUNE 2013

Impact Factor: 2.69 · DOI: 10.1021/jp402745m · Source: PubMed

CITATION

1

READS

16

8 AUTHORS, INCLUDING:



[Raghavan Rajagopalan](#)

Covidien

33 PUBLICATIONS 707 CITATIONS

SEE PROFILE



[Yuefei Shen](#)

University of Massachusetts Medical School

13 PUBLICATIONS 223 CITATIONS

SEE PROFILE



[Amolkumar Karwa](#)

Mallinckrodt

16 PUBLICATIONS 144 CITATIONS

SEE PROFILE



[John-Stephen A. Taylor](#)

Washington University in St. Louis

153 PUBLICATIONS 6,412 CITATIONS

SEE PROFILE

Roles of Free Radicals in Type 1 Phototherapeutic Agents: Aromatic Amines, Sulfenamides, and Sulfenates

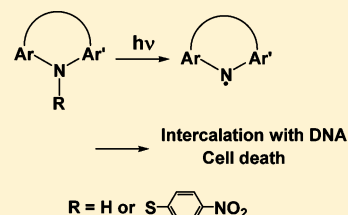
Tien-Sung Lin,^{*,†} Raghavan Rajagopalan,[‡] Yuefei Shen,[†] Sungho Park,[†] Amruta R. Poreddy,[‡] Bethel Asmelash,[‡] Amolkumar S. Karwa,[‡] and John-Stephen A. Taylor[†]

[†]Department of Chemistry, Washington University, St. Louis, Missouri 63130, United States

[‡]Covidien Pharmaceuticals, 675 McDonnell Boulevard, Hazelwood, Missouri 63042, United States

S Supporting Information

ABSTRACT: Detailed analyses of the electron spin resonance (ESR) spectra, cell viability, and DNA degradation studies are presented for the photolyzed Type I phototherapeutic agents: aromatic amines, sulfenamides, and sulfenates. The ESR studies provided evidence that copious free radicals can be generated from these N–H, N–S, and S–O containing compounds upon photoirradiation with UV/visible light. The analyses of spectral data allowed us to identify the free radical species. The cell viability studies showed that these agents after exposure to light exert cytotoxicity to kill cancer cells (U937 leukemia cell lines HTC11, KB, and HT29 cell lines) in a dosage- and time-dependent manner. We examined a possible pathway of cell death via DNA degradation by a plasmid cleavage assay for several compounds. The effects of photosensitization with benzophenone in the presence of oxygen were examined. The studies indicate that planar tricyclic amines and sulfenamides tend to form π -electron delocalized aminyl radicals, whereas nonplanar ones tend to yield nitroxide radicals resulting from the recombination of aminyl radicals with oxygen. The ESR studies coupled with the results of cell viability measurements and DNA degradation reveal that planar N-centered radicals can provide higher potency in cell death and allow us to provide some insights on the reaction mechanisms. We also found the formation of azatropylium cations possessing high aromaticity derived from azepines can facilitate secondary electron transfer to form toxic $O_2^{\bullet-}$ radicals, which can further exert oxidative stress and cause cell death.

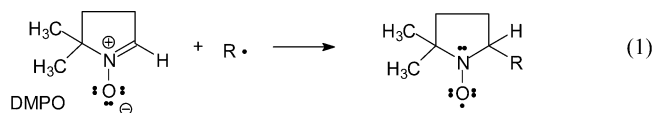


1. INTRODUCTION

Recently we reported on the therapeutic efficacy studies of two classes of photolabile agents: aromatic sulfenamides (S–N containing agents)¹ and tricyclic diarylamines,² which were classified as Type 1 phototherapeutic agents. These compounds generated copious free radicals upon photoexcitation with UV/visible light as observed in our electron spin resonance (ESR) studies. The photoinduced radicals are assigned to N-centered and S-centered radicals in sulfenamides and to N-centered radicals in amines. These photolyzed compounds have been shown to cause cell death in a dosage- and time-dependent manner. However, the corresponding sulfenates (S–O containing agents) were inactive despite the fact that these compounds also generated a substantial amount of free radicals (assigned as S-centered and O-centered radicals) upon photoirradiation. In subsequent studies to be present in this article, we attribute the phototherapeutic effects of these agents mainly to the presence of N-centered radicals and their reactions with substrates. Among the sulfenamides and amines, we found their therapeutic efficacy varied with respect to molecular structures. We postulated that the therapeutic potency of nitrogen-containing aromatic molecules is related to the specific types of free radical generated upon photoirradiation.

Some of the photoinduced organic free radicals are reactive and short-lived. These nascent free radicals can recombine or undergo electron transfer to convert the surrounding substrates

to other reactive species. For these compounds, we employed a spin trapping agent, DMPO (5,5-dimethyl-1-pyrroline-N-oxide), to trap the short-lived radical species. The DMPO spin adducts are relative stable nitroxides with long enough lifetimes for ESR measurements. The DMPO spin adducts have unique spectral patterns depending on the type of free radicals (R^\bullet) added to the 2-position (β -carbon) of DMPO (see eq 1).^{3,4} Thus, ESR spin trapping experiments allow us to identify the short-lived free radicals generated upon photoirradiation.



In some cases, the photogenerated N-centered free radicals from these compounds can further react with O_2 to form stable nitroxides, which do not require a spin trapping agent for ESR measurements. In other cases, the ESR spectra can become extremely broadened as a result of the paramagnetic effect of dissolved O_2 . However, if the solution is deoxygenated by purging with nitrogen gas, the spectra become sharp, displaying well-resolved characteristics of ^{14}N and proton hyperfine splitting.⁵

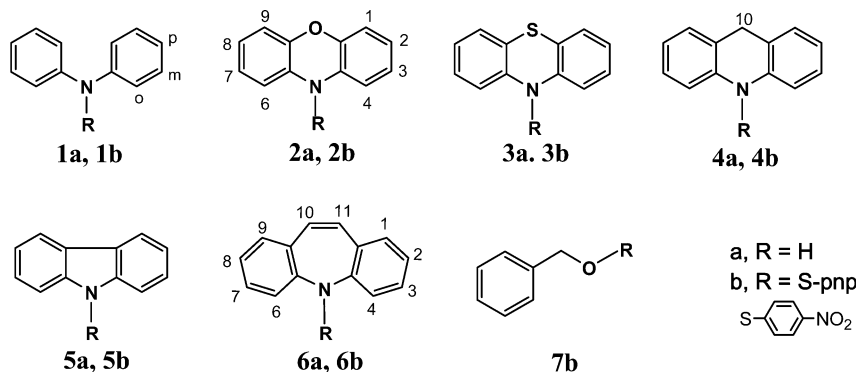
Received: March 20, 2013

Revised: May 31, 2013

Published: June 5, 2013



Chart 1. Structures of Amine (N–H), Sulfenamide (N–S), and Sulfonate (S–O) compounds



In this study, we report the analyses of ESR spectra of aromatic compounds containing N–H, N–S, and S–O chemical bonds (Chart 1), which are susceptible to photo-fragmentation; i.e., the cleavage of N–H bond in amines, N–S bond in sulfenamides, and S–O bond in sulfonates. The ESR spectral analyses and the DNA degradation studies of these structurally similar compounds allow us to elucidate reaction mechanisms and their cytotoxicity observed in the cell viability study. Our current study further allows us to establish the structure–activity relationships of these agents after photo-irradiation.

2. EXPERIMENTAL SECTION

2.1. Sources of Chemicals. Aromatic sulfenamides and sulfonates were prepared according to the standard procedures given previously;^{1,2} the spin trapping agent DMPO (5,5-dimethyl-1-pyrroline-*N*-oxide) was purchased from Alexis Biochemical Co. (now EnzoLife Sciences, NY), and aromatic amines were purchased from Aldrich Chemical Co. (St. Louis, MO), except acridane (9,10-dihydro-acridine) from Chem Pacific (Baltimore, MD).

2.2. Plasmid Cleavage. The 2.7 kb (kilo base pair) plasmid pHOT1 (20 μ g/mL) was, respectively, mixed with acridane (1 mM, 100 μ M, and 0) in PBS buffer to make samples of a total volume of 20 μ L (31 μ M DNA bp). Samples were then exposed under UV light (BLAK-RAY, Model B 100 AP, 365 nm) for 10 and 20 min. After mixing with 6 \times loading buffer, samples were subjected to 1% agarose gel electrophoresis and visualized by staining with ethidium bromide. Band intensities of supercoiled form (Form I) and open circular form (Form II) were quantified with Quantity One Software and then converted to fraction of Form I taking into account the decreased stainability of Form I DNA by a factor of 1.22. The number of strand breaks per plasmid could then be calculated from $\ln(\text{fraction Form I})$.⁶

2.3. Cell Viability Studies. The procedures and details of cell viability measurements were given previously.^{1,2}

2.4. ESR Studies. An X-band ESR spectrometer (Joel FA 100) was employed in our studies. The Joel rectangular resonator has a 0.5-in hole in the front for light access. The settings of the spectrometer used in our measurements are as follows: microwave frequency, 9.2–9.5 GHz; power, 2–5 mW (less than 1 mW for samples with narrow line width); and modulation width, 0.01–0.05 mT. The g values of free radicals were determined by the following formula:

$$g_x - g_{\text{std}} = -\frac{(B_x - B_{\text{std}})}{B_{\text{std}}} g_{\text{std}}$$

where g_x is the g value of the unknown sample, and g_{std} is the g value of standard sample.⁷ We used Fremy's salt (KSO_3)₂NO as the standard, which has a g value of 2.0055. However, the uncertainty (average of several runs) is ± 0.0005 , so the g values are expressed to four significant figures.

A 100 W tungsten/halogen lamp was used as the irradiation source. The actual incident power density on the sample was not determined as we were only interested in the relative ESR intensity and the characterization of free radical generated under the same photoirradiation conditions. However, the actual power density for cell viability studies was measured precisely as 4 J/cm² (see refs 1 and 2 for details). The power density of the light source used in the DNA degradation measurement was the same as that used in the cell viability study. We used Pyrex tubing as the sample tube in the measurements, which filtered out the UV region of the light source. The lifetime measurements on the light-sensitive signal of the spin adduct were performed by sitting the external field on the top of a signal, and using the “time scan” mode instead of the “field scan” mode of the spectrometer.

Over 50 photolabile compounds with various functional groups were studied (detailed structures of 51 compounds were given as Figure S1 in the Supporting Information). The preparation and spectral characterization of these compounds were given previously.^{1,2} Approximately 50 mM stock solutions of the target compounds and 100 mM DMPO (both in benzene) were prepared. A mixture containing equal volumes of the target compound stock solution and the DMPO solution (150 μ L each) was placed in a sample tubing (4 mm OD). ESR was recorded before, during, and after photoirradiation to examine its effect. All experiments were performed at room temperature. Before irradiation, weak background ESR signals were observed in some samples. However, some of the amines have been shown to produce stable nitroxide radicals or aminyl radicals with relatively long lifetimes⁵ that would not require spin trapping agents in our ESR measurements.

Since the concentration of dissolved oxygen in a benzene solution is about 1 mM, it would have caused line broadening in the observed ESR spectra. For comparison, the solution was purged with nitrogen gas for 5 min (flow rate: 50 mL/min). The sample tube was capped with a rubber septum with two hypodermic needles inserted (inlet and outlet) during the gas purging. After purging, the needles were removed and the sample remained sealed with the septum under N₂ atmosphere during the ESR measurements.

3. RESULTS AND DISCUSSION

The results of the ESR measurements and DNA degradation studies are presented below. The results of our ESR studies of 13 compounds are presented first in order to demonstrate the nature of photoinduced free radicals from aromatic amines, sulfenamides, and sulfenates, followed by the discussion of structure–activity relationships in terms of the photogenerated free radicals, cell viability, and DNA degradation.

3.1. Nitrogen-Centered Radicals. The photoirradiation of tricyclic diarylamines and the corresponding sulfenamides can yield N-centered radicals in one or more of the following three forms: (1) aminyl radicals (neutral N-centered radicals) generated from the cleavage of N–H or N–S bond, (2) cation radicals ($>\text{NH}^{\bullet+}$) by ionization or photooxidation, or (3) stable nitroxide radical ($>\text{N}-\text{O}^{\bullet}$) by a subsequent reaction of an aminyl radical with oxygen.⁸ These radicals may further recombine to form diamagnetic molecules. The presence of cation radicals can be ruled out in our cases, as the visible wavelength of irradiation does not have the energy high enough to ionize or to photo-oxidize the amines, and there is no oxidizing agent present in the solution to remove an electron from the amines. Three aspects of the nitrogen-containing radicals are discussed in the following sections.

3.1.1. Aminyl Radicals. Upon photolysis, all tricyclic diarylamines and sulfenamides produce aminyl radicals with different yields and stability. In some cases, photoinduced aminyl radicals are reactive and readily react with oxygen to form nitroxides, such as diphenylamine (1a) and diphenylsulfenamide (1b) (vide infra). Figure 1 shows the ESR spectra of

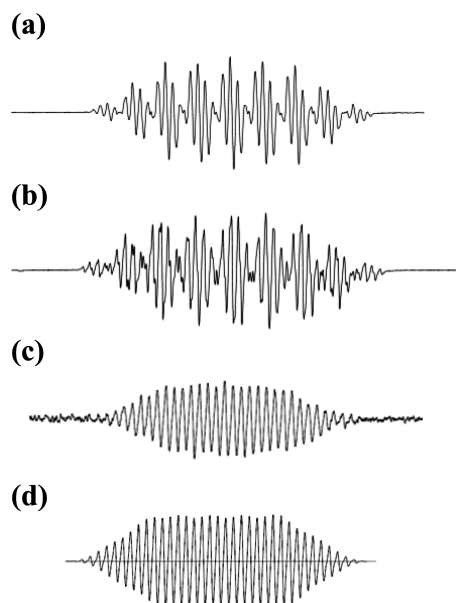


Figure 1. ESR spectra of aminyl radicals observed in deoxygenated photolyzed samples without using a spin trapping agent: (a) phenoxazine aminyl radical from phenoxazine (2a) with the following parameters, $g = 2.002 (\pm 0.0005)$; $a_{\text{N}} = 0.78$ mT, $a_{\text{H}3,\text{H}7} = 0.38$ mT, $a_{\text{H}1,\text{H}9} = 0.31$ mT, $a_{\text{H}2,\text{H}8} = 0.10$ mT, $a_{\text{H}4,\text{H}6} = 0.07$ mT, and $\sigma(\text{fwhh}) = 0.016$ mT; (b) from phenoxazine sulfenamides (2b), same parameters as panel a; (c) from azepine (6a), $g = 2.002 (\pm 0.0005)$; and (d) simulated spectrum of panel with the following parameters, $a_{\text{N}} = 0.84$, $a_{\text{H}(2)} = 0.42$, $a_{\text{H}(4)} = 0.22$, $a_{\text{H}(4)} = 0.11$ mT; the numbers in the parentheses refer to the number of equivalent protons. Detailed assignments are given in Table 1.

photolyzed phenoxazine (2a), azepine (6a), and the corresponding sulfenamides (2b). We observed well-resolved hyperfine splitting from ^{14}N and protons of the phenyl rings only in the deoxygenated samples. Note that the observed spectra of the photolyzed deoxygenated 2a and 2b are identical (Figures 1a and 1b). These two ESR spectra clearly show that photolysis cleaves the N–H bond in secondary aromatic amines and the N–S bond in sulfenamides. The counter S-centered radicals generated from sulfenamides were not observed as they were reactive and short-lived; hence, they can only be observed in the presence of a spin trapping agent (vide infra). The spectral parameters of phenoxazine and azepine aminyl radicals are summarized in Table 1. These hyperfine splittings are the same as those reported previously.^{8,9} The following spectral parameters were used to simulate the spectra of azepine (6a) (compare Figures 1c and 1d): $g = 2.002 (\pm 0.0005)$, $a_{\text{N}} = 0.84$, $a_{\text{H}(2)} = 0.42$, $a_{\text{H}(4)} = 0.22$, and $a_{\text{H}(4)} = 0.11$ mT. The numbers given in the parentheses indicate the number of equivalent protons. The assignments given in Table 1 are based on the spin density distribution of anthracene-type radicals. We also observed aminyl radicals in the photolysis of compounds 4a and 5a (vide infra).

3.1.2. Nitroxide Radicals. The aminyl radicals can further react with oxygen to form nitroxide radicals if the sample is not deoxygenated during irradiation. The resulting spectral lines are greatly broadened due to the paramagnetic effect of oxygen. However, we observed sharp and well resolved hyperfine patterns after purging the solution with nitrogen gas. Figure 2 shows the ESR spectra of photolyzed compounds 1a and 3a. This is the typical spectral pattern for aromatic nitroxides. The spectral parameters of diphenylnitroxide derived from the photolysis of diphenylamine (1a) are given in Table 1. The hyperfine splittings are the same as those reported for diphenylnitroxide.^{5,10}

We note a contrasting behavior between phenoxazine (2a) and phenothiazine (3a) upon photolysis: 2a generates predominantly the aminyl radical, whereas 3a produces predominately the nitroxide. This effect may arise from molecular rigidity;¹¹ i.e., the phenyl rings in 2a are in the same molecular plane but not in phenothiazine. Furthermore, it is noted that compound 6a (azepine) also produces an aminyl radical predominantly as shown in Figure 1c, and that 6a is a planar species according to a quantum mechanical calculation using Spartan software. However, phenothiazine is a twisted nonplanar molecule with C_s symmetry, but its aminyl radical is planar with C_{2v} symmetry according to the Spartan calculation. The stability of these aminyl radicals may arise from the greater degree of delocalization (resonance) of the unpaired electron in rigid planar molecules. Recently, it was further pointed out that the difference in dissociation energy (BDE) of the N–H bond might also dictate the fate of dissociation products. The BDE values for amines were given as follows: 1a (diphenylamine) 85.8 > 3a(phenothiazine) 79.3 > 2a (phenoxazine) 77.2 kcal/mol.⁸ Thus, it seems that compounds with higher BDE and nonplanarity tend to form nitroxide radicals.

3.1.3. DMPO Spin Adducts of Aminyl Radicals. For some amines, such as acridane (4a) and carbazole (5a), since the steady concentration of aminyl radicals upon irradiation with visible light were too low to be detected by direct ESR measurements, DMPO was employed in the studies. The detected signals were attributed to DMPO/PhN $^{\bullet}$ spin adducts, where Ph is referred to an aromatic moiety with substantial π bonding, which can stabilize the free radical. The spectra of

Table 1. ESR Paramagnetic Parameters of Photolyzed Samples

compound	type of radical detected	g (± 0.0005)	a_N (mT) (± 0.01)	a_H (mT) ^a (± 0.01)
1a	nitroxide	2.006	0.98	$a_{H\alpha} = a_{H\beta} = 0.19$ $a_{Hm} = 0.09$
1b	DMPO/RS [•]	2.004	1.32	$a_{H\beta} = 1.32$
2a	aminyl	2.002	0.78	$a_{H3,H7} = 0.38$ $a_{H1,H9} = 0.31$ $a_{H2, H8} = 0.10$ $a_{H4,H6} = 0.07$ same as above for 2a
2b	aminyl	2.002	0.78	
3a	nitroxide	2.005	0.82	$a_{H1,H9} = 0.29$ $a_{H2,H8} = 0.09$
4a	DMPO/PhN [•]	2.004	1.42	2.11
4b	DMPO/RS [•]	2.004	1.32	$a_{H\beta} = 1.32$
5a	DMPO/PhN [•]	2.004	1.45	2.11
6a	aminyl	2.002	0.84	$a_{H10,H11} = 0.42$ $a_{H1,H4,H6,H9} = 0.22$ $a_{H2,H3,H7,H8} = 0.11$ $a_{H\beta} = 1.32$
7b	DMPO/RS [•]	2.004	1.32	

^aSee Chart 1 for the numbering of protons at the adjacent carbon position.

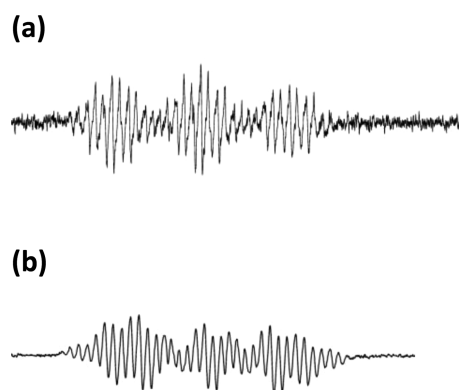


Figure 2. ESR spectra of nitroxide radicals observed in photolyzed samples in the presence of oxygen as a result of the reaction between aminyl radicals and oxygen. The spectra were obtained after light irradiation and the subsequent deoxygenation to ensure sharper spectral line width: (a) diphenylnitroxide from diphenylamine (**1a**) with the following paramagnetic parameters, $g = 2.006$ (± 0.0005), $a_N = 0.98$ mT, $a_{H\alpha} = a_{H\beta} = 0.19$ mT, and $a_{Hm} = 0.09$ mT; and (b) phenothiazine (**3a**), $g = 2.005$ (± 0.0005), $a_N = 0.82$ mT, $a_{H1,H9} = 0.29$ mT, and $a_{H2,H9} = 0.09$ mT.

photolyzed **4a** and **5a** in the presence of DMPO were given previously,² and they are further displayed as Figure S3 in Supporting Information for easy comparison. Both of these two compounds give DMPO/PhN[•] spin adducts with slightly different spectral parameters as given in Table 1. The value of $a_{N\beta}$ is too small to be measured due to the fact that the unpaired π -electron is greatly delocalized into the aromatic rings. Also, a small amount of residual oxygen after deoxygenation may further broaden the spectral lines. We note that ¹⁴N splitting in the aliphatic N-centered DMPO spin adducts (DMPO/[•]NMe₂) was reported to have a value of only 0.19 mT.¹²

3.2. Sulfur-Centered Radicals (Thiyl Radicals). Sulfur-centered radicals (thiyl radicals) generated in the photolysis of sulfenamides and sulfenates were elusive and could not be detected without the assistance of DMPO. The ESR spectra of photolyzed **1b** and **7b** in the presence of DMPO are shown in Figure 3. These spectra consist of two radical components: (1)

a set of signals with weaker intensity and longer lifetime is assigned to an N-centered stable DMPO/PhN[•] spin adduct for compound **1b** and to an O-centered DMPO/RO[•] spin adduct in **7b**; (2) the other strong component with a shorter lifetime is assigned to an S-centered DMPO/RS[•] spin adduct (RS[•] phenyl thiyl radical). Both compounds **1b** and **7b** generate the same S-centered radicals as clearly demonstrated in Figure 3. The signal centered at 327.53 mT ($g = 2.004$), which has a relatively high intensity, is short-lived and formed instantaneously upon irradiation. The hyperfine splitting parameters of this strong signal were $a_N = a_{H\beta} = 1.32$ mT. The intensity ratio of this signal is roughly 1:2:2:1. At first glance, this spectral pattern looks like a typical pattern of the DMPO/HO[•] spin adduct.^{4,13} However, we noticed that our measured g and hyperfine values are smaller than those of the reported values for the DMPO/HO[•] spin adduct: $g = 2.005$, and $a_N = a_{H\beta} = 1.49$ mT.¹³ Moreover, our ESR signal disappeared within 1 min after turning off the light source, in contrast to DMPO/HO[•] spin adducts, which are generally stable over several hours. The time profiles of the fast decaying signals are shown in Figure 4d,h. The strong signal grew and reached the steady state within 5 s, and the average decay half-life was about 10 s, while the counterpart DMPO/PhN[•] adduct in compound **1b** had a weaker intensity and a lifetime of several hours.

The spectral parameters of DMPO/RS[•] have been reported as $g = 2.006$ (± 0.0005), $a_N = 1.29$ mT, and $a_{H\beta} = 1.41$ mT from the photolysis of diphenyl disulfide dissolved in toluene.¹⁴ Our measured values are about the same as the reported values within experimental uncertainties. The spectral parameters of the DMPO/RS[•] spin adduct are given in Table 1. The lifetime difference between DMPO/RS[•] and DMPO/PhN[•] spin adducts further allows us to assign these two sets of spectra unambiguously.

In a recent study, the decay and formation of the DMPO/RS[•] spin adduct has been reported,¹⁵ where RS[•] was generated in the photocleavage of nitrosothiol:



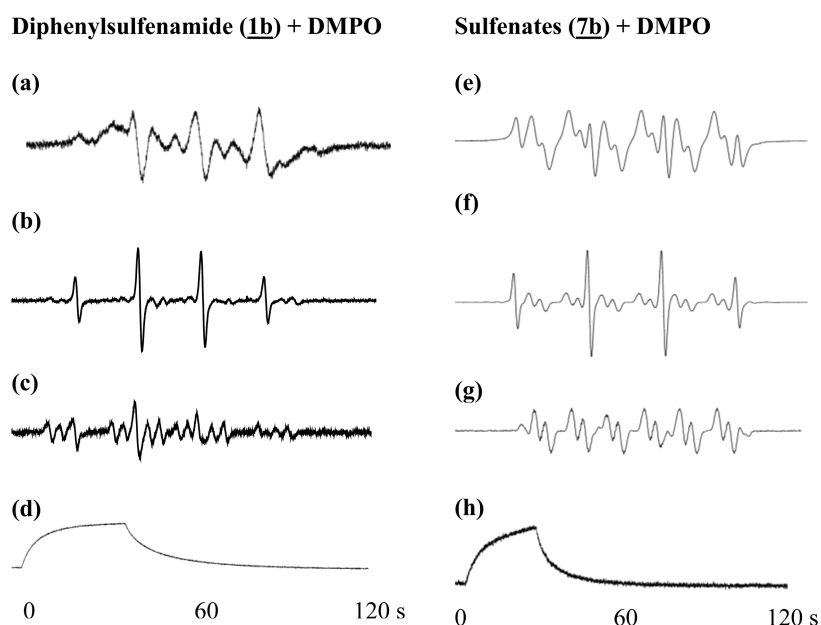


Figure 3. ESR spectra of DMPO spin adducts of photolyzed diphenylsulfenamide (**1b**) and sulfenates (**7b**): (a) for **1b** sample taken in the presence of oxygen; (b) deoxygenated sample during light irradiation, the strong peaks are assigned to S-centered spin adducts (DMPO/RS[•]); (c) irradiated sample **b** taken in the dark, 2 min after irradiation, here the weak signals are assigned to N-centered spin adducts (DMPO/PhN[•]); (d) rise and decay time profile of S-centered spin adducts taken at the second strongest peak. The time scale is 2 min; (e) for sulfenate (**7b**) sample in the presence of oxygen; (f) deoxygenated sample during irradiation; (g) after irradiation, taken in the dark, here the weak signals are assigned to O-centered spin adduct; and (h) the rise and decay of DMPO/RS[•] spin adducts taken at the second strong peak (326.61 mT). Note that the spectral similarity between spectra **b** and **f** as both strong peaks arise from the same DMPO/RS[•] spin adducts.

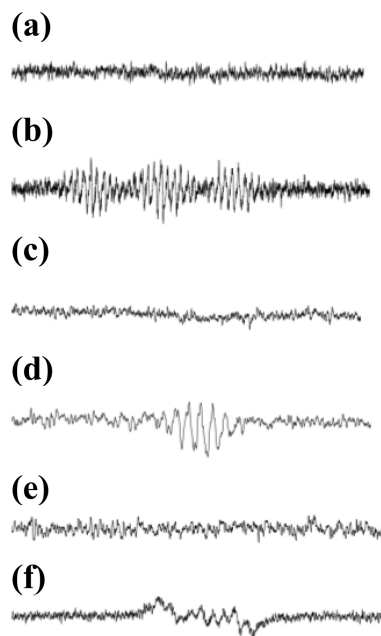


Figure 4. ESR spectra of photolyzed deoxygenated samples to examine the effect of photosensitization by benzophenone in the absence of DMPO: (a) diphenylamine (**1a**), 15 min irradiation with tungsten lamp, no noticeable signal was observed; (b) with an addition of equal volume of 50 mM benzophenone solution, deoxygenated, spectrum was recorded after 2 min of irradiation with light. Similar effects were observed in acridane (**4a**): (c) untreated sample, 8 min irradiation, no signal; (d) in the presence of benzophenone, spectrum was recorded after 3 min of irradiation; in carbazole (**5a**), (e) untreated sample, 10 min irradiation, no signal; and (f) in the presence of benzophenone, spectrum was recorded after 4 min of irradiation.

The forward rate constant of reaction (3) was given as $2.6 \times 10^8 \text{ M}^{-1} \text{ s}^{-1}$ and dissociative backward rate constant as $0.3 \text{ M}^{-1} \text{ s}^{-1}$. These values are consistent with the time profile of our measurements: fast DMPO spin adduct formation and slower decay time of $\sim 10 \text{ s}$. The assignment of the S-centered spin adduct is further confirmed in other photolyzed sulfur-containing compounds.

We note there is a nitro group in all sulfenamides we have studied. It has been reported that nitrobenzene upon photoexcitation to the $^3n\pi^*$ state can undergo rearrangement to form hydroxylamine by hydrogen abstraction.^{16,17} The hydroxylamine may further be broken down in the subsequent photolysis and release an OH[•] radical to form a DMPO/OH[•] spin adduct, which is known to be stable over several hours at room temperature. However, the presence of the OH[•] radical can be ruled out in our system based on the hyperfine splitting constant and lifetime of the DMPO/OH[•] 1:2:2:1 signal.

3.3. Photosensitization and Oxygen Effects. In some of the compounds, the yield of steady-state free radicals upon photoirradiation is too low to be measured by ESR experiments if a spin trapping agent is not employed. For instance, no noticeable ESR signal was observed in the sample of diphenylamine dissolved in benzene (50 mM) after 15 min of irradiation with a tungsten lamp (Figure 4a). This is consistent with the result of a previous report that the efficiency of photodissociation of diphenylamine in benzene is relatively low.⁵ However, upon addition of 50 μL of 50 mM benzophenone solution to 150 μL of 50 mM diphenylamine solution, a substantial yield of free radicals was observed. The ESR spectrum of the photolyzed sample in the presence of benzophenone, the spectrum recorded after 2 min of irradiation, is displayed in Figure 4b, which is identical to the reported spectrum of diphenylnitroxide.⁵

Similar photosensitization effects by benzophenone were also observed in other aromatic amines, as shown in Figures 4c and 4d for **4a** (acridane) and in Figures 4e and 4f for **5a** (carbazole). The ESR spectra of the photoinduced free radicals from compounds **4a** and **5a** are of aminyl radical type. The enhancement effect is attributed to the triplet photosensitization of benzophenone.^{5,18,19} As the triplet quantum yield of benzophenone is near unity, it can efficiently transfer its energy to the triplet state of the target molecule and thereby induce a photochemical reaction even though the irradiation wavelength is below their λ_{max} 's (300 nm for acridane and 340 nm for carbazole).¹¹

As mentioned previously, we observed spectral broadening in the presence of oxygen. To examine the effects of oxygen, we studied the spectral patterns before and after purging the solution with nitrogen gas for 5 min. Typical spectra are displayed in Figure 5. Before purging, a very broad spectrum

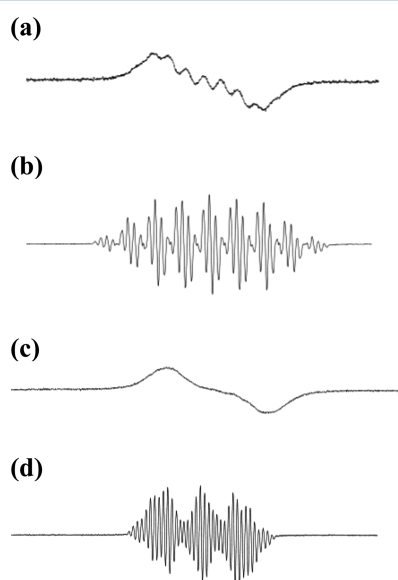


Figure 5. ESR spectra of photolyzed samples to examine the oxygen effect in the absence of DMPO: (a) phenoxazine (**2a**) in the presence of oxygen; (b) sample a was deoxygenated, and the spectrum was taken during irradiation, aminyl radical signal; (c) phenothiazine (**3a**) in the presence of oxygen; and (d) sample c was deoxygenated, and the spectrum was taken during irradiation, a typical aromatic nitroxide signal.

was observed as shown in Figure 5a,c; after purging, the spectra became sharp and exhibited well-resolved hyperfine splittings of ^{14}N and protons (see Figure 5b,d). A similar oxygen effect was also observed in the DMPO spin adducts (see Figure 3a,e). Furthermore, an electron transfer from the photogenerated free radicals to O_2 to form $\text{O}_2^{\bullet-}$ may further broaden the signal of the newly generated free radical upon photolysis. However, if the oxygen present in the solution is minimal and can react with aminyl radicals to form stable nitroxides, then slight line

broadening would be observed as reported for photolyzed diphenylamine dissolved in super cooled molten benzophenone, which gave well resolved proton splittings.⁵

3.4. Cell Death and DNA Degradation. In previous studies, we had demonstrated that some of the photolyzed aromatic amines and sulfenamides can effectively induce cell death.^{1,2} The results of cell viability measurements are summarized in Table 2. The cell death may be caused by DNA degradation and/or other causes, such as lipid peroxidation or cell membrane damage by oxidative stress. It is known that the introduction of one single-strand DNA break can easily cause the conversion of supercoiled (Form I) to open circular form (Form II). Thus, we examined the degree of conversion of Form I of pHOT1 plasmid to Form II in the presence of these Type 1 phototherapeutic agents under UV exposure. Figure 6 displays band intensities of agarose gel

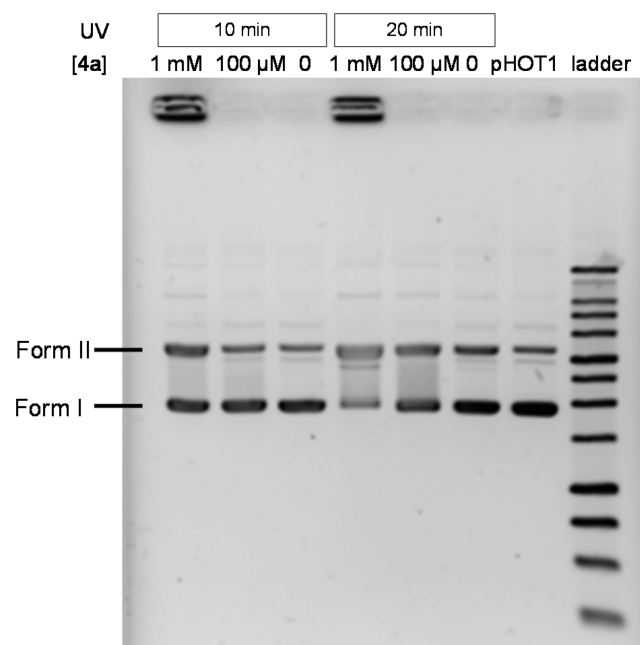


Figure 6. Band intensities of agarose gel electrophoresis for supercoiled form (Form I) and open circular form (Form II) of pHOT1 plasmid by acridane (**4a**) under UV exposure.

electrophoresis for supercoiled form (Form I) and open circular form (Form II) of pHOT1 plasmid for compound **4a**, which showed the most photocleavage of all the agents tested. The number of strand breaks per plasmid DNA induced by **4a** in the presence of UV light, and in excess of UV light alone, is summarized in Table 3. Note that 1 mM acridane was able to induce 0.72 strand breaks per plasmid corresponding to one break per 3.75 kb when exposed to UV light for 20 min, which dropped to 0.25 (1 break per 11 kb) when the irradiation time was reduced to 10 min. When the concentration of **4a** was reduced 10-fold to 100 μM , the number of strand breaks per

Table 2. Summary of Cell Viability (IC_{50}) of Targeted Agents

Sample	1a	1b	2a	2b	3a	3b	4a	4b	5a	5b	6a	6b	7b
IC_{50} (μM) ^a	N.D. ^b	6.8 \pm 1.3	14.5 \pm 1.54	>20	1.39 \pm 0.11	12.4 \pm 1.2	0.68 \pm 0.11	1.3 \pm 1.2	5.56 \pm 1.15	>20	2.58 \pm 1.14	1.2 \pm 1.1	N.D. ^b

^aAverage of at least 3 independent runs. ^bNot determined due to the lack of difference between dark and phototoxicity at the entire concentration range.

Table 3. Quantitation of the Number of Strand Breaks Per Plasmid, *S*, Induced by Acridane (4a) and 365 nm Light As Deduced from Analysis of the Conversion of Supercoiled Form (Form I) to Open Circular Form (Form II) of pHOT1 Plasmid

UV exposure	acridane concentration	Form I (%)	<i>S</i> ^a	increase in <i>S</i> due to acridane
10 min	1 mM	59	0.53	0.25
	100 μ M	71	0.34	0.05
	0	75	0.28	
20 min	1 mM	33	1.1	0.72
	100 μ M	59	0.53	0.15
	0	68	0.38	
none	0	76	0.28	

^aThe number of single strand breaks per plasmid, *S*, was calculated from $\ln(\text{fraction Form I})$ taking account of the reduced stainability of Form I DNA.

plasmid induced by 4a and UV light was 0.15 (1 break/18 kb) with a 20 min exposure and 0.05 (1 break/10 kb) with a 10 min exposure. Less but significant cleavage was also observed with compound 4b, showing 0.2 strand breaks (1 break/13.5 kb) at 1 mM concentration for 20 min, though the cleavage was barely detectable for the 10 min exposure. However, little photocleavage was observed when compounds 1a, 3a, 5a, 6a, and 6b were examined. Of these, 6b showed the most cleavage at 1 mM for 20 min (0.09 or 1 break/30 kb), but no cleavage was observed at the 10 min exposure (data not shown). This is in accord with the higher IC_{50} values for 1a, 3a, 5a, 6a, and 6b of N.D., 1.39, 1.30, 5.56, 2.58, and 1.20 μM , respectively, compared to 0.68 μM for compound 4a (Table 2). In the following section, we will attempt to provide plausible reaction mechanisms and possible pathways of cell death based on the spectral characterization of free radicals generated during photodissociation.

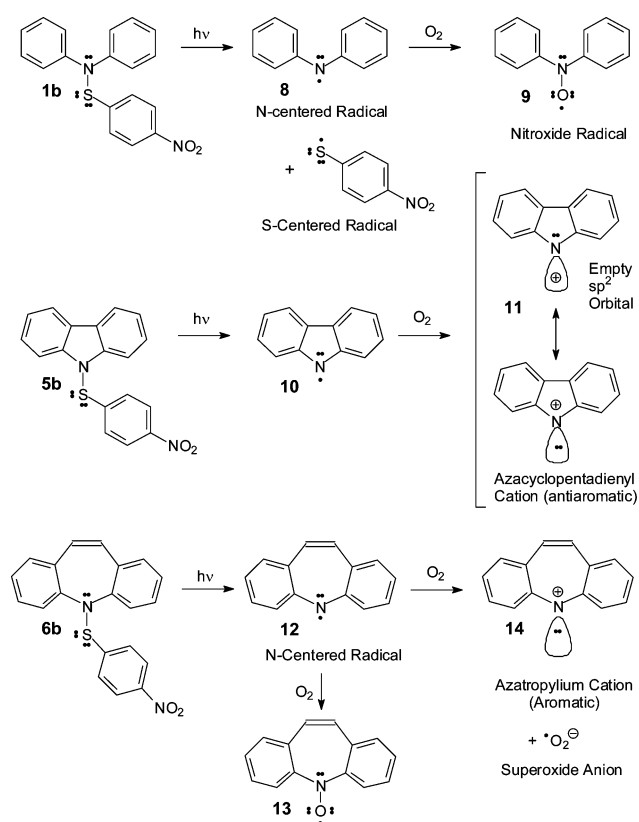
3.5. Reaction Mechanism, Cell Viability, and Structural Relationship. Our cell viability and ESR studies demonstrated that N-centered free radicals generated from photolysis of Type 1 phototherapeutic agents are responsible for cell death. The results of cell viability measurements of these compounds are summarized in Table 2. We shall focus our discussion on the tricyclic diarylamines and the corresponding sulfenamides. Analyses of the ESR spectra of these two classes of structurally similar compounds allow us to identify the final products, to assess the stability of intermediates, to propose a possible mechanistic rationale of photochemical reactions, and to establish activity–structure relationship.

First, we discuss the possible mechanisms of photochemical reactions for aromatic sulfenamides (**b** compounds) only, as the corresponding amines are simply the replacement of the *p*-nitrophenyl group of sulfenamide with hydrogen. The reaction can be rationalized by two possible mechanisms shown in Scheme 1.

(1) For nonplanar molecules, such as diphenylamines and sulfenamides (compound 1) and phenothiazine (compound 3), the end products are predominantly of nitroxide type (shown as product 9 in Scheme 1).

(2) For planar molecules, aminyl radicals are formed shown as products 10 and 12 in Scheme 1. We note that the azatropylium cation (14) intermediates generated from 5*H*-dibenzo[*b,f*]azepine (6a) and 5-(4-nitrophenylthio)dibenzo-

Scheme 1. Proposed Photochemical Reaction Mechanism of Aromatic Sulfenamides



[*b,f*]azepine (6b) possess high aromaticity and stability. The stable azatropylium cation would favor an electron transfer from the aminyl radical (12) to O_2 , and subsequently form $\text{O}_2^{\bullet-}$, which can exert oxidative stress to cells. In contrast, oxidation of 10 produced from the carbazole compounds (5a and 5b) would produce a much less stable cation as judged from the possible resonance isomers. The π lone pair isomer would have an empty sp^2 orbital, whereas the σ lone pair isomer results in an antiaromatic azacyclopentadienyl cation (11), and therefore, 10 is unlikely to transfer an electron to form $\text{O}_2^{\bullet-}$. We would therefore expect carbazoles to exert less cytotoxicity, which is consistent with our cell viability studies.^{1,2}

Second, we examine the varying effects of different free radicals on cell viability and summarize the findings as follows:

(1) The nitrogen-centered free radicals are responsible for cell death based on the following two observations: (a) all sulfenamides (**b** type molecules) produce the same S-centered radical, but cell viability was observed to be very different among various sulfenamides; (b) same S-centered (*p*-nitrophenylthiyl) radicals were generated in compound 7b (sulfenamide) and all sulfenamide compounds, but 7b showed no activity at all.

(2) Planar molecules have higher activity than nonplanar ones; e.g., acridanes (4) have higher activity than diphenylamine and diphenylsulfenamide.

(3) Compounds with high aromaticity in reaction intermediates give higher activity than those that do not have stable intermediates, e.g., 6 (azepine) is more active than 5 (carbazole) (see Scheme 1).

(4) Amines (**a** type) and the corresponding sulfenamides (**b** type) have comparable activity, even though amines give

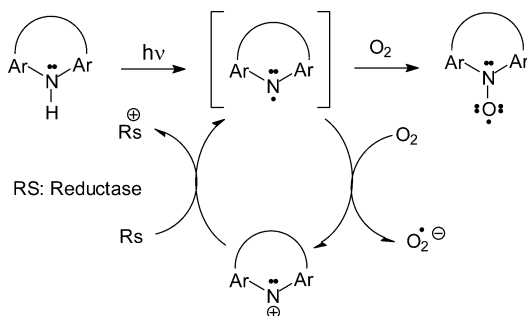
slightly higher activity than sulfenamides with one slight exception of compound **6** (azepine). This effect may arise from the better intercalation of the amines with DNA than that of the sulfenamides. Note that the bulky sulfenamide group may introduce nonplanarity to the molecular geometry. Previously, acridines and proflavine (planar N-containing tricyclic planar aromatic compounds) have been reported to favor intercalation with DNA.^{20,21} The free radicals generated upon irradiation in these planar compounds are stabilized by intercalation with DNA and may therefore induce DNA cleavage and provide higher activity in cell death.

From the laser transient studies of these compounds in solution, the lifetimes of nascent radicals are on the order of several nanoseconds to microseconds.²² In order to cause cell death effectively by the free radical mechanism, these nitrogen-containing aromatic molecules may have to intercalate with DNA of cells via π stacking. Then, the nascent free radicals generated by photoirradiation of the sample would be stabilized and lengthened in lifetime by intercalation, giving ample time for single strand breakage to take place through abstraction of hydrogens from the DNA, thereby leading to cell death.^{23–25} This proposed mechanism is demonstrated in the current DNA degradation tests for which irradiation of 1 mM **4a** in the presence of 31 μ M bp of DNA caused 1 strand break per 3.75 kb. The DNA base pair concentration in a spherical human cell of 10 μ m in diameter can be estimated to be 22 mM, and thus, one could expect significant chromosomal DNA strand cleavage at the IC₅₀ of 0.68 μ M observed for compound **4a**.

Another plausible pathway involves fast electron transfer to oxygen from the initially photochemically generated intermediates that can form stable intermediates such as the azatropylium cation species with high aromaticity, species **14** in Scheme 1. The resulting reactive oxygen species (ROS), such as superoxide anion radicals ($\text{O}_2^{\bullet-}$), hydroxyl ($\bullet\text{OH}$), and/or hydroperoxyl radicals, have been shown to be cytotoxic and are responsible for cell death and injury.^{23,25,26}

Furthermore, in the presence of a cellular reductase (such as thioredoxin), the relatively stable azatropylium cation may recycle back to an aminyl radical and creating a cyclic process (Scheme 2) that produces superoxide anion radicals and exerts

Scheme 2. Fate of Nitrogen Centered Radicals in the Presence of Cellular Enzyme (Thioredoxin Reductase) and Oxygen to Execute Possible Multiple Hits of ROS



oxidative stress to cellular components as proposed for hypoxia-selective, bioreductive drugs.²³ This is especially relevant in the discussion of selective cell death of tumor cells by free radical mechanisms. We speculate all planar N-centered radicals can follow this cyclic pathway and exert oxidative stress to cellular

components of tumor cells and that the presence of a reductases may play an important role in tumor cell death.

4. CONCLUSIONS

We have employed ESR techniques to study free radicals generated from more than 50 aromatic secondary amine, sulfenamide, and sulfenate compounds upon UV/visible irradiation. The studies provide evidence that copious free radicals can be generated from these N–H, N–S, and S–O containing aromatic compounds upon photoirradiation. The planar aromatic amines and sulfenamides tend to form aminyl radicals (via π -electron delocalization), while the nonplanar ones tend to yield nitroxide radicals (via recombination with oxygen). The ESR studies coupled with the results of cell viability measurements reveal that planar N-centered (aminyl) radicals have high potency in cell death. The most potent ones are compounds **4** and **6**. Cytotoxicity demonstrated by these free radicals may arise from an intercalation of aromatic planar N-centered free radicals with DNA, which causes single strand breakage as demonstrated in our DNA degradation studies. We further propose two possible pathways to gauge the activity of these free radicals: (1) planar molecules provide π conjugation to stabilize the N-centered radicals and allow for molecular stacking in DNA segments, similar to G \cdots C and A \cdots T base pairings, and (2) aromatic intermediates, such as tropylium cations derived from azepines, can facilitate secondary electron transfer to form toxic $\text{O}_2^{\bullet-}$ radicals, which can further cause cell death. The latter pathway would be important if cellular reductases are present, which can lead to an interconversion of aminyl radicals and tropylium cations, generating an abundance of ROS and selectively inducing cell death of tumor cells.²³

■ ASSOCIATED CONTENT

Supporting Information

Chemical structures, simulated spectra, and ESR spectra. This material is available free of charge via the Internet at <http://pubs.acs.org>.

■ AUTHOR INFORMATION

Corresponding Author

* (T.-S.L.) Fax: 314-935-4481. E-mail: lin@wustl.edu.

Notes

The authors declare no competing financial interest.

■ ACKNOWLEDGMENTS

We thank Prof. Richard Loomis and Drs. Jeng-Jong Shieh, Richard B. Dorshow, James Kostelc, Gary Cantrell, and David Pipes for helpful discussions.

■ REFERENCES

- (1) Karwa, A. S.; Poreddy, A. R.; Asmelash, B.; Lin, T.-S.; Dorshow, R. B.; Rajagopalan, R. Type I Phototherapeutic Agents: Preparation and Cancer Cell Viability Studies of Novel Photolabile Sulfenamides. *ACS Med. Chem. Lett.* **2011**, 2, 828–833.
- (2) Rajagopalan, R.; Lin, T.-S.; Karwa, A. S.; Poreddy, A. R.; Asmelash, B.; Dorshow, R. B. Type I Phototherapeutic Agents, Part II: Cancer Cell Viability and ESR Studies of Tricyclic Diarylamines. *ACS Med. Chem. Lett.* **2012**, 3, 284–288.
- (3) Janzen, E. G. Spin Trapping. *Acc. Chem. Res.* **1971**, 4, 31–35.
- (4) Janzen, E. G. Radical Addition Reactions of 5,5-Dimethyl-1-pyrroline-1-oxide. ESR Spin Trapping with a Cyclic Nitron. *J. Magn. Reson.* **1973**, 9, 510–512.

- (5) Lin, T.-S.; Retsky, J. ESR Studies of Photochemical Reactions of Diphenylamines, Phenothiazines and Phenoxazines. *J. Phys. Chem.* **1986**, *90*, 2687–2689.
- (6) Hertzberg, R. P.; Dervan, P. B. Cleavage of Double Helical DNA by Methidium-propyl-EDTA-Iron(II). *J. Am. Chem. Soc.* **1982**, *104*, 313–315.
- (7) Weil, J. A.; Bolton, J. R.; Wertz, J. E. *Electron Paramagnetic Resonance*; Wiley-Interscience: New York, 1994.
- (8) Lucarini, M.; Pedrielli, P.; Valgimigli, G. F. P.; Gimes, D.; Tordo, P. Bond Dissociation Energies of the N–H Bond and Rate Constants for the Reaction with Alkyl, Alkoxy, and Peroxyl Radicals of Phenothiazines and Related Compounds. *J. Am. Chem. Soc.* **1999**, *121*, 11546–11553.
- (9) Baird, J. C.; Thomas, J. R. Electron Paramagnetic Resonance Spectra of Some Disubstituted Nitric Oxides. *J. Chem. Phys.* **1961**, *1961*, 1507–1508.
- (10) Lin, T. S. EPR Study of Diphenylnitroxide in Benzophenone. *J. Chem. Phys.* **1972**, *57*, 2260–2264.
- (11) Brede, O.; Maroz, A.; Hermann, R.; Naumov, S. Ionization of Cyclic Aromatic Amines by Free Electron Transfer: Products Are Governed by Molecule Flexibility. *J. Phys. Chem. A* **2005**, *109*, 8081–8087.
- (12) Migita, C. T.; Migita, K. Spin Trapping of the Nitrogen-Centered Radicals. Characterization of the DMPO/DEPMPO Spin Adducts. *Chem. Lett.* **2003**, *32*, 466–467.
- (13) Finkelstein, E.; Rosen, G. M.; Rauckman, E. J. Spin Trapping. Kinetics of the Reaction of Superoxide and Hydroxyl Radicals with Nitrones. *J. Am. Chem. Soc.* **1980**, *102*, 4994–4999.
- (14) Mile, B.; Rowlands, C. C.; Sillmana, P. D.; Fildes, M. The EPR Spectra of Thiyl Radical Spin Adducts Produced by Photolysis of Disulfides in the Presence of 2,4,6-Tri-*tert*-butylnitrosobenrene and 5,5-Dimethyl-1-pyrroline N-Oxide. *J. Chem. Soc., Perkin Trans. 2* **1992**, 1431–1437.
- (15) Potapenko, D. I.; Bagryanskaya, E. G.; Tsentalovich, Y. P.; Reznikov, V. A.; Khramtsov, T. L. C. V. Reversible Reactions of Thiols and Thiyl Radicals with Nitrone Spin Traps. *J. Phys. Chem. B* **2004**, *108*, 9315–9324.
- (16) Hurley, R.; Testa, A. C. Photochemical $n\rightarrow\pi^*$ Excitation of Nitrobenzene. *J. Am. Chem. Soc.* **1966**, *88*, 4330–4335.
- (17) Hurley, R.; Testa, A. C. Nitrobenzene Photochemistry. II. Protonation in the Excited State. *J. Am. Chem. Soc.* **1967**, *89*, 6917–6921.
- (18) Turro, N. J.; Ramamurthy, V.; Scaiano, J. C. *Principles Of Molecular Photochemistry*; University Science Books: Sausalito, CA, 2009.
- (19) Simons, J. P. *Photochemistry and Spectroscopy*; Wiley-Interscience: New York, 1971.
- (20) Wilson, W. D.; Ratmeyer, L.; Strekowski, M. Z.; Boykin, D. The Search for Structure-Specific Nucleic Acid-Interactive Drugs: Effects of Compound Structure on RNA versus DNA Interaction Strength. *Biochemistry* **1993**, *32*, 4098–4104.
- (21) Ames, B. N.; Gurney, E. G.; Miller, J. A.; Bartsch, H. Carcinogens as Frameshift Mutagens: Metabolites and Derivatives of 2-Acetylaminofluorene and Other Aromatic Amine Carcinogens. *Proc. Natl. Acad. Sci. U.S.A.* **1972**, *69*, 3128–3132.
- (22) Shukla, D.; Rege, F. D.; Wan, P.; Johnston, L. J. Laser Flash Photolysis and Product Studies of the Photoionization of N-Methylacridan in Aqueous Solution. *J. Phys. Chem.* **1991**, *95*, 10240–10246.
- (23) Wardman, P.; Dennis, M. F.; Everett, S. A.; Pate, K. B.; Stratford, M. R. L.; Tracy, M. Radicals from One-electron Reduction of Nitro Compounds, Aromatic N-oxides and Quinones: The Kinetic Basis for Hypoxia-selective, Bioreductive Drugs. *Biochem. Soc. Symp.*; Royal Chem. Soc.: 1995; Vol. 61, pp 171–194.
- (24) Wang, J.; Rivas, G.; Luo, D.; Cai, X.; Valera, F. S.; Dontha, N. DNA-Modified Electrode for the Detection of Aromatic Amines. *Anal. Chem.* **1996**, *68*, 4365–4369.
- (25) Kehler, J. P. Free Radicals as Mediators of Tissue Injury and Disease. *Crit. Rev. in Toxicol.* **1993**, *23*, 21–48.
- (26) Dugan, L. L.; Lin, T.-S.; He, Y. Y.; Hsu, C. Y.; Choi, D. Detection of Free Radicals by Microdialysis/Spin Trapping EPR Following Focal Cerebral Ischemia Reperfusion and a Cautionary Note on the Stability of 5,5-Dimethyl-1-pyrroline N-Oxide (DMPO). *Free Radical Res.* **1995**, *23*, 27–32.